Supporting Information

for

Anionic *sod*-type Terbium-MOF with Extra-Large Cavities for Effective Anthocyanin Extraction

Wei Du,[a] Zhifeng Zhu,[a] Yue-Ling Bai,[a,b] Zhen Yang,[a] Shourong Zhu,[a] Jiaqiang Xu,*[a] Zhaoxiong Xie,[b] and Jianhui Fang[a]*

[a]Department of Chemistry, College of Science, Shanghai University, Shanghai 200444 (China)

[b]State Key Laboratory for Physical Chemistry of Solid Surfaces and Department of Chemistry, College of Chemistry and Chemical Engineering, Xiamen University, Xiamen 361005 (China)

Experimental Section

All starting materials and solvents were purchased commercially and used without purification except for H_6TATAT, which was synthesized according to the literature[1] with minor modifications. IR spectra were recorded in the range of 400-4000 cm^{-1} on a Nicolet Avatar-370 spectrometer. The elemental analyses (CHN) were performed with German elemental analyzer Vario ELIII. The thermogravimetric analysis was performed with a STA409PC instrument. The X-ray powder diffraction patterns were collected by a Rigku D/max-2200. The adsorption spectra were performed with a PUXI TU-1900 UV-vis spectrometer. The solid-state emission spectra were measured on a Shimadzu RF-5310. Crystallographic data were collected with a Bruker D8 Venture ($Cu_{k\alpha}$= 1.54178 Å). CCDC: 1820611.

Synthesis of **H_6TATAT**: 0.084 mol 5-aminoisophthalic acid, 0.134 mol NaOH and 0.104 mol $NaHCO_3$ were added into 140 mL H_2O in a round-bottomed flask, the mixture was stirred at 0 °C for 30 min, then 70 mL 1,4-dioxane containing 0.02 mol cyanuric chloride was slowly added with constant stirring. The final mixture was refluxed at 110 °C for 24 h. After cooling to room temperature, the solution was adjusted to pH = 1 with concentrated HCl. 11.55 g white solid was collected by centrifugation, washed with distilled water and EtOH, and dried in air (yield: 94 %). ^{1}H NMR ([D6]DMSO, 500 MHz): δ=8.12 (3H), 8.47 (6H), 9.68 (3H), 13.0 (6H) ppm.

Synthesis of compound **1**: A mixed solvent of DMA (8 mL) and H_2O (4 mL) containing H_6TATAT (0.05 mmol), $Tb(NO_3)_2{\cdot}6H_2O$ (0.10 mmol) and concentrated nitric acid (0.2 mL) was stirred for half an

hour at room temperature. Then the solution was transferred to a 23 mL Teflon-lined stainless steel vessel and heated at 130 °C for 2 days. After cooling down to room temperature, pale yellow solution was filtered and the solution was evaporated for one week at room temperature. Pale yellow polyhedral crystals of compound **1** were obtained, washed with DMA and dried in the air. Yield: 25.8 mg (37.4 %). Calcd for $C_{130}H_{167}N_{34}Cl_3O_{68}Tb_6$ (found): C, 35.86 (35.63); H, 3.87 (3.94); N, 10.94 (10.95).

Single-crystal studies:

Crystallographic data of **1** was collected on a Bruker D8 Venture ($Cu_{k\alpha}$ = 1.54178 Å). The structure was solved by direct methods and refined by full-matrix least-squares calculations (F^2) using SHELXTL-14 software and Olex2 1.2 software.[2,3] All non-H atoms were refined in the anisotropic approximation against F^2 for all reflections. Some H atoms of the coordinated H_2O molecules could not be located, but they were included in the formula. Because guest molecules ($(CH_3)_2NH_2^+$) in the channels were highly disordered and could not be modeled properly, the SQUEEZE routine of PLATON was applied to remove their contributions to the scattering. The reported refinements are of the guest-free structures obtained by the SQUEEZE routine, and the results were attached to the CIF file. PLATON/SQUEEZE[4] were employed to calculate their contributions to the distorted molecules and given a set of guest-free diffraction intensities. The structure was then refined again using the generated data. Crystallographic data of **1** is summarized in **Table S1**.

The X-ray diffraction pattern and thermal gravimetric analysis:

The powder X-ray diffraction (PXRD) pattern of the as-synthesized compound matched well with the simulated one, indicating that the polycrystalline sample is pure phase (Fig. S4). And the crystals of compound **1** are stable and insoluble in water and common organic solvents (Fig. S5). In order to investigate the stabilities of their cages, the samples were activated by solvent-exchange with water and ethanol, respectively. The thermal gravimetric analysis of as-synthesized, ethanol activated and water soaked **1** were investigated under a nitrogen atmosphere, respectively. The curve of as-synthesized **1** shows a gradual weight loss process; no obvious platforms appeared in the range of 25~800 °C. While the water-soaked sample of **1** exhibits a rapid weight loss process of 22.16 % between 25 and 140 °C, corresponding to the removal of all protonated dimethylamine, Cl^- ions, guest solvent molecules and coordinated water (*ca.* 21.83%). An obvious plateau appears and the framework is stable to ~480 °C, then the frameworks begin to decompose rapidly. The curve of ethanol-activated **1** is similar to the water-soaked sample and the framework can be also stable to ~480 °C (Fig. S7). This result indicates the anionic frameworks of water-soaked and ethanol-activated **1** can remain intact and have an excellent thermal stability. Unfortunately, the BET surface area failed to be calculated through the N_2 adsorption/desorption experiments, presumably because the cages were blocked by the free $[(CH_3)_2NH_2]^+$ cations and/or the extra-large cavities in the frameworks lost their long-range order under high vacuum activation.[5]

Table S1. Crystallographic data for **1**.

Compound	**1**
Molecular formula	$C_{130}H_{167}N_{34}Cl_3O_{68}Tb_6$
Fw	4353.8155
Temperature,*T* / K	173(2)
crystal system	cubic
space group	*Fm-3c*
a, Å	54.8796
b, Å	54. 8796
c, Å	54. 8796
V, Å^3	165284.72
Z	192
D, g/cm^{32}	0.599
F(000)	28944
R_{int}	0.1414
$R_1{}^a$, wR_2 [$I > 2\sigma(I)$]	$R_1 = 0.0668$; $wR_2 = 0.2059$
$R_1{}^a$, wR_2 (all data)	$R_1 = 0.0767$; $wR_2 = 0.2182$
Goodness-of-fit,	1.131

Reference:

1 X. Zhao, H. He, T. Hu, F. Dai and D. Sun, *Inorg. Chem.*, 2009, **48**, 8057–8059.

2 G. M. Sheldrick, *Acta Crystallogr. Sect. C Struct. Chem.*, 2015, **71**, 3–8.

3 O. V. Dolomanov, L. J. Bourhis, R. J. Gildea, J. A. K. Howard and H. Puschmann, *J. Appl. Crystallogr.*, 2009, **42**, 339–341.

4 A. L. Spek, *J. Appl. Crystallogr.*, 2003, **36**, 7–13.

5 M. J. Dong, M. Zhao, S. Ou, C. Zou and C. De Wu, *Angew. Chemie Int. Ed.*, 2014, **53**, 1575–1579.

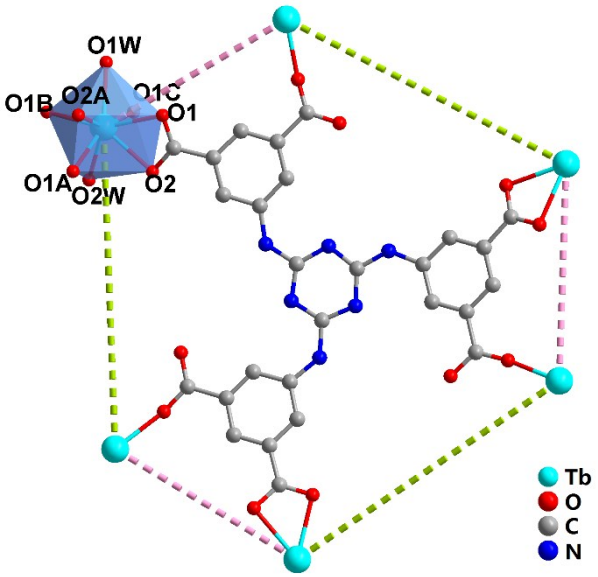

Fig. S1 The coordination model of $TATAT^{6-}$ ligand and TbO_8 hendecahedron unit of **1**. H atoms have been omitted for clarify. Colour code: Tb, cyan; O, red; N, blue; C gray.

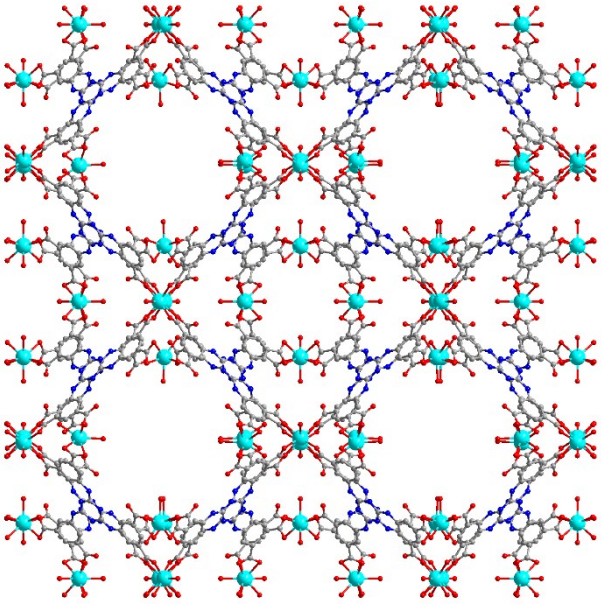

Fig. S2 The 3D network of **1** viewed along a/b/c axis. Guest molecules, water molecules and H atoms have been omitted for clarify. Colour code: Tb, cyan; O, red; N, blue; C gray.

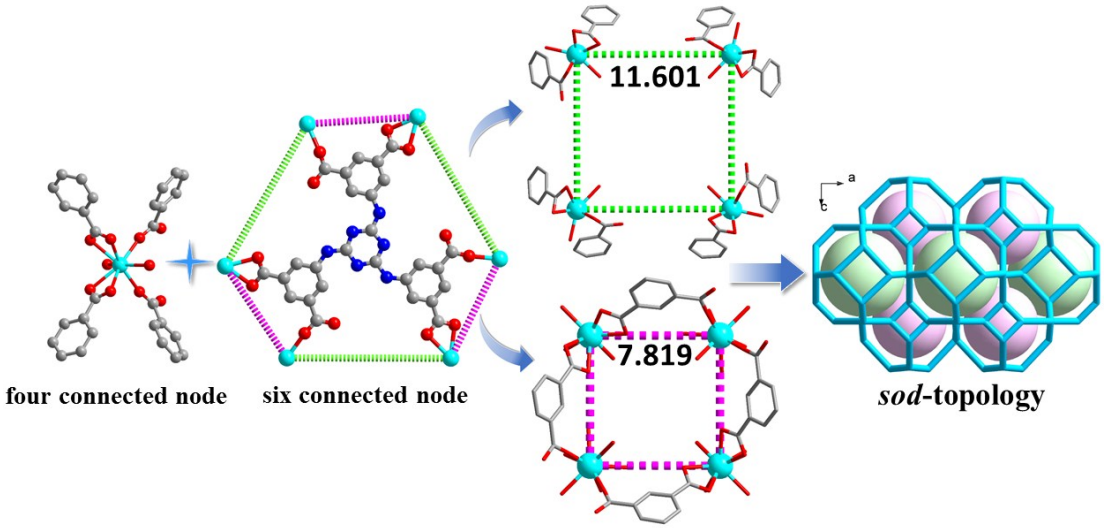

Fig. S3 The coordination environment of Tb^{3+} ion and the coordination model of $TATAT^{6-}$ ligand, larger and smaller rectangle window, and the 3D *sod*-type network. Guest molecules, water molecules and H atoms have been omitted for clarify. Colour code: Tb, cyan; O, red; N, blue; C gray.

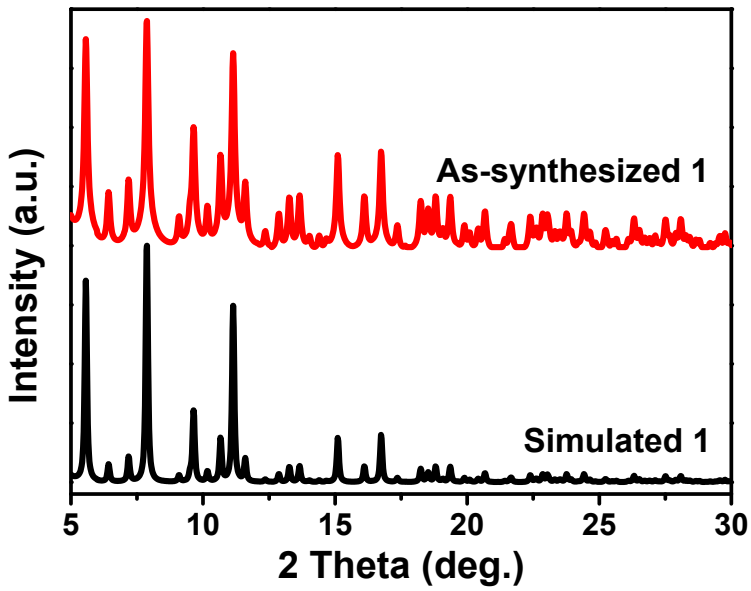

Fig. S4 The experimental and simulated PXRD diffraction patterns of compound **1**.

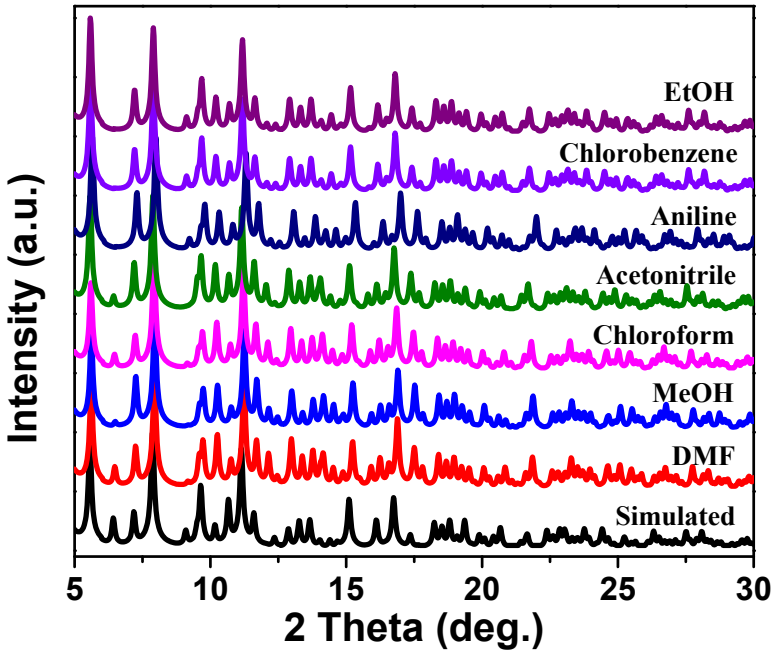

Fig. S5 The PXRD diffraction patterns of **1** soaked in common solvents for 24 h.

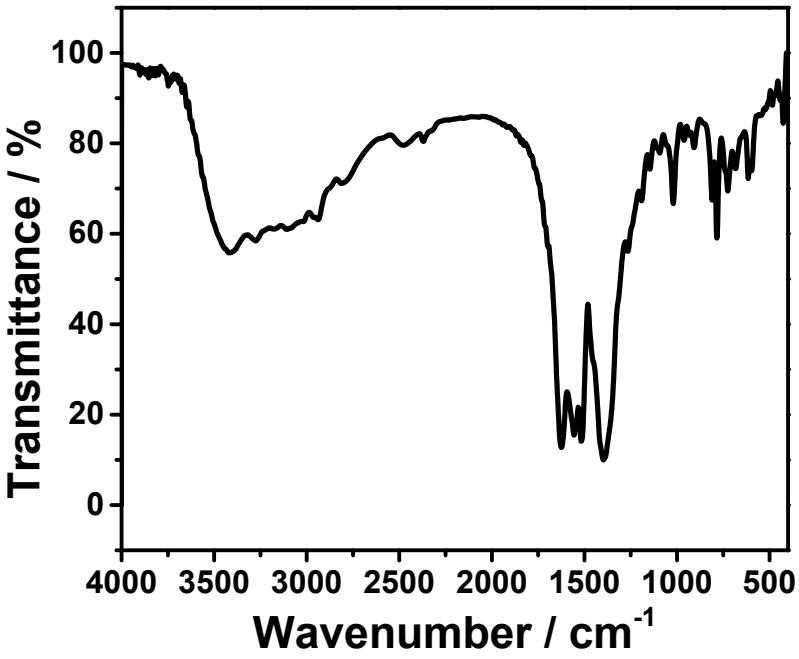

Fig. S6 IR spectra of compound **1**.

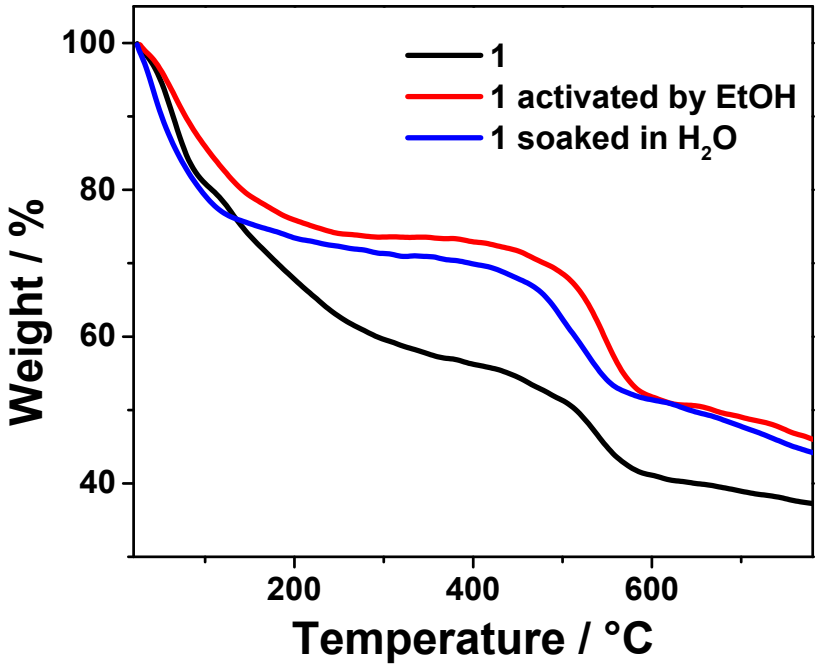

Fig. S7 TGA curve got in a N_2 atmosphere with a heating rate of 10 °C min^{-1} for compound **1**, water-soaked sample **1** and EtOH-soaked sample **1**, respectively.

Adsorption experiment of cyanidin chloride: The adsorption ability of compound **1** was evaluated by adsorb cyanidin chloride (**Cy·Cl**) ethanol solution at room temperature. 10 mg compound **1** was added in 10 mL of 8 mg/L **Cy·Cl** ethanol solution in a 20 mL glass bottle by shaking in an oscillator continuously for 84 h. The clear solution was transferred into a 1 cm quartz cell to measure UV-vis spectra from 300 nm to 800 nm on a PUXI TU-1900 UV-vis spectrometer (stray light < 0.01%; wavelength accuracy, 0.3 nm). Absolute ethanol was used as reference in this experiment.

The maximum adsorption capacity was estimated by adding 10 mg compound **1** into 10 mL of 8 g/L **Cy·Cl** ethanol solution for 12 h. Then, washed compound **1** with ethanol and weighed after drying. Repeat the above steps to ensure the weight does not change.

Adsorption and recycling experiments of blackberries solution: Since the experimental blackberry was purchased directly from the market, and the natural instability of the plant itself, the UV-Vis spectra of blackberry solution is slightly different. 0.5 g blackberries were immersed in 50 mL deionized water for 1 h and lavender solution was obtained after filtration. To verify the main component of the obtained solution is anthocyanins, the filtrate was divided into multiple portions and the volume of each portion was 2 mL to adjust pH = 3, 5, 7, 8, 9 and 11. The results show that the solution in different pH values show different colors, pink in acidic condition and blue in alkaline condition, indicating that natural anthocyanins in blackberries dissolved in water (Fig. S8). In order to study the effect of anionic framework **1** on the extraction of natural anthocyanins, the pH of experiment solution was adjusted to 5. Three solutions (2 mL) with different initial absorbance value of about 0.5, 1.5 and 2.0 are prepared, respectively. 10 mg compound **1** was added into 2 mL blackberry solution by shaking for a while. The clear solution was transferred into a 1 cm quartz cell to measure UV-vis spectra from 300 nm to 800 nm on a PUXI TU-1900 UV-vis spectrometer (stray light < 0.01%; wavelength accuracy, 0.3 nm). The adsorption rate is 79.26 % for the solution with an absorbance of 0.5, 43.72 % for that of 1.5 and 34.38 % for that of 2.0 at 30 min, which reveals that the adsorption rate increases with decreasing concentration. Although the adsorption rate is slow in high-concentration solution, the adsorption capacity increases with time.

The cyclic experiments were performed by adding 30 mg compound **1** into 2 mL blackberry solution by shaking in an oscillator continuously for 30 min. Filter the crystals and then add into 10 mL NaCl aqueous/ethanol mixed solution by shaking for 30 min. Filter the crystals again and wash with ethanol

for several times. Dry the sample and proceed to the next cycle. As shown in Fig.19, the first adsorption rate can reach 73.08 %, the second adsorption rate decreases slightly, and its value is 65.68 %. However, the third and fourth adsorption rates decrease significantly, with values of 35.74 % and 15.97 %, respectively. The decreased sorption rate indicates that Na^+ ions cannot fully exchange **C3G**$^+$ ions during the release process.

The maximum adsorption capacity was estimated by adding 10 mg compound **1** into 10 mL of saturated **BB** solution for 12 h. Then, washed compound **1** with ethanol and weighed after drying. Repeat the above steps to ensure the weight does not change.

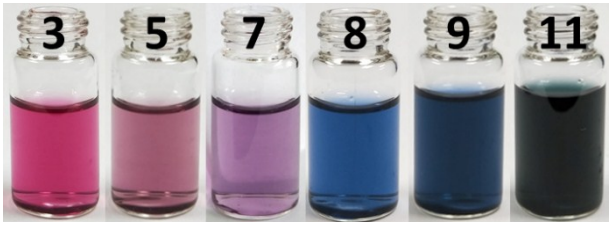

Fig. S8 The color change of blackberries solution at different pH.

Fig. S9 The photos of crystals **1** before (left) and after (right) soaking in blackberries aqueous solution.

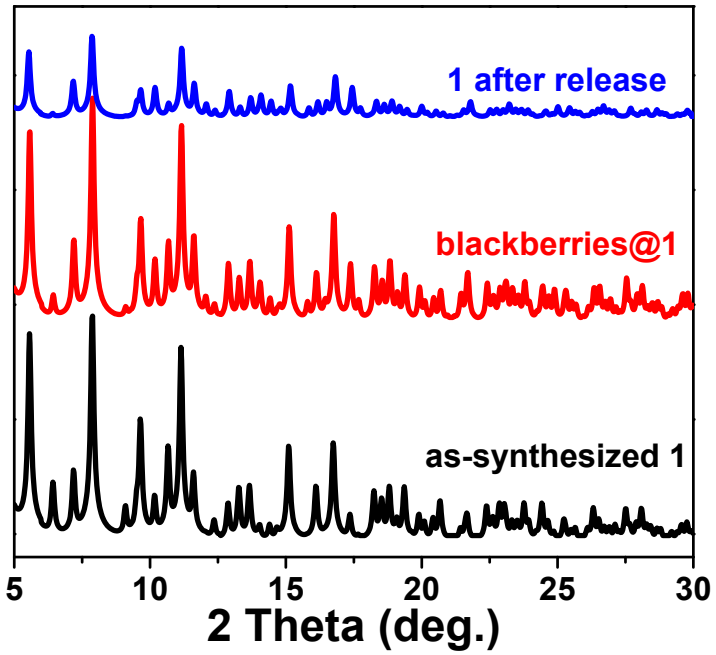

Fig. S10 The PXRD diffraction patterns of **1**, blackberries **@1** and **1** after release.

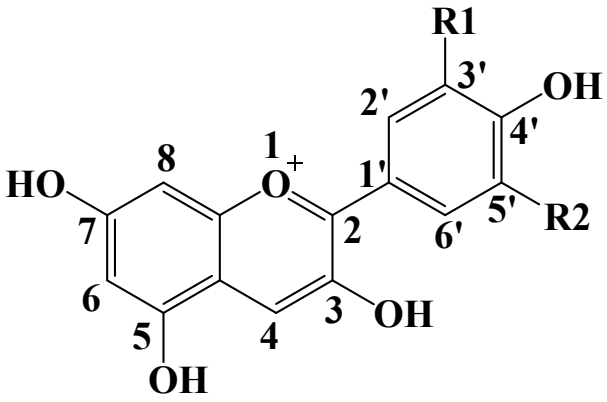

Anthocyanin	R_1	R_2
Pelargonidin	H	H
Cyanidin	OH	H
Delphinidin	OH	OH
Peonidin	OCH_3	H
Petunidin	OCH_3	OH
Malvidin	OCH_3	OCH_3

Fig. S11 The main structures of anthocyanidins in food.

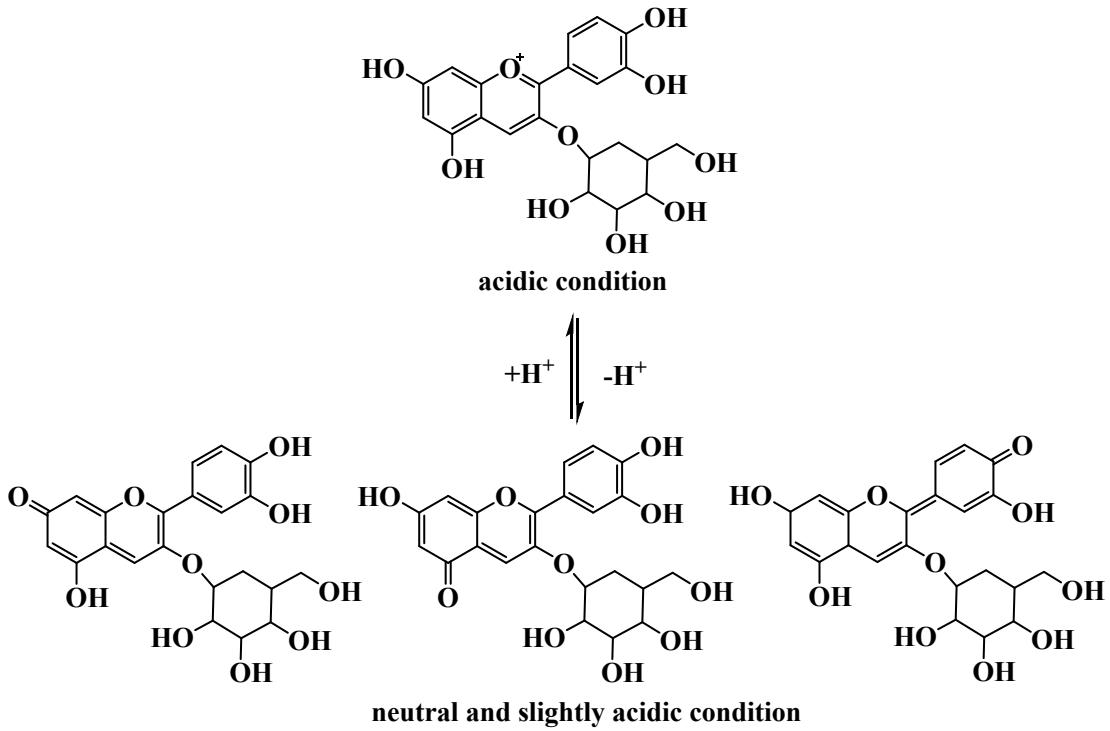

Fig. S12 The structures of cyanidin-3-O-glucoside (**C3G**) under neutral and acidic conditions, respectively.

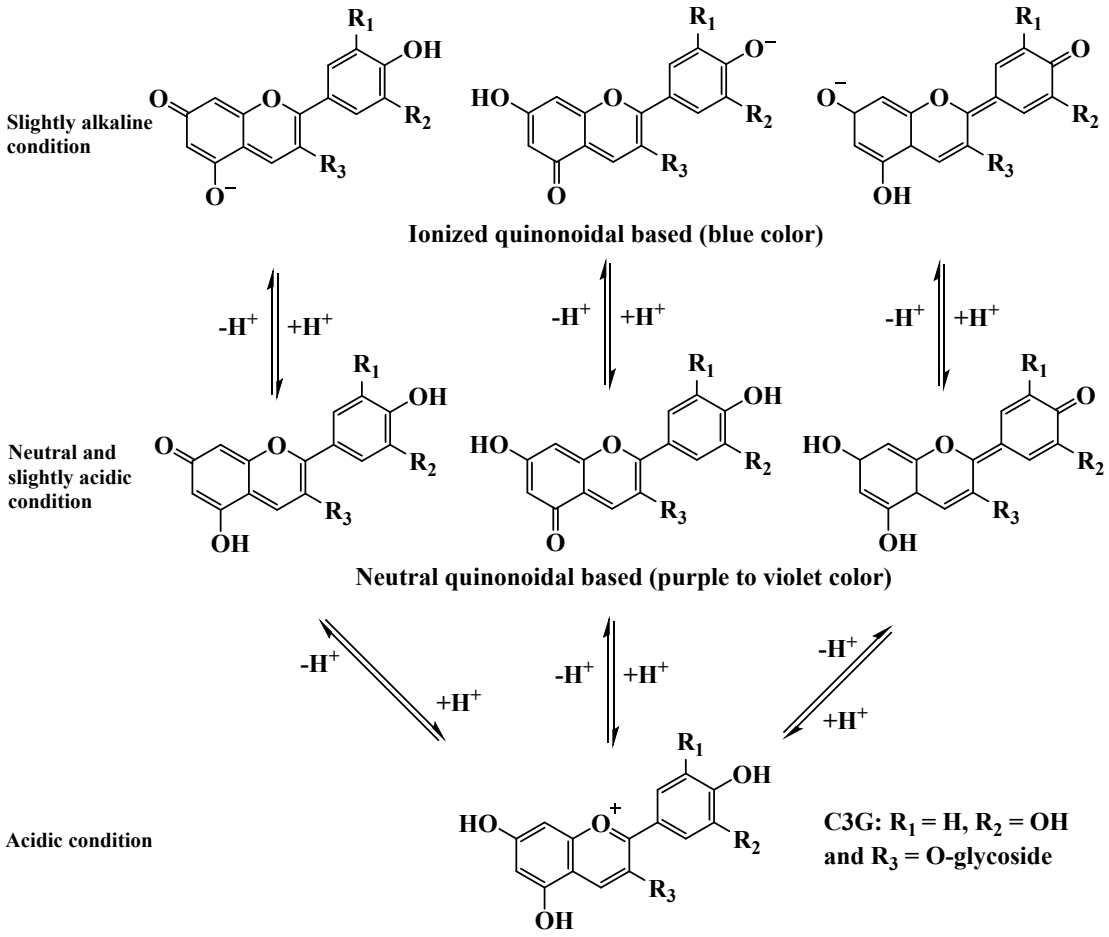

Fig. S13 Conformations of anthocyanins in aqueous solution under different pH.

Theoretical calculation: The adsorption simulations for Na^+ and **C3G**$^+$ were performed with Accelrys Materials Studio 7.0 using the universal force field method. Before the simulation, the structure of cyanidin-3-glucoside (**C3G**$^+$) molecular was firstly optimized in DMol3 module using generalized gradient approximation with the Perdew-Burke-Ernzerof exchange correlation, to get an optimal conformation. The simulations of adsorption isotherms and energy distribution curves were carried out in the Sorption module, with 10 fugacity steps using configurational bias method at temperature of 298 K.

Fig. S14 and S15 show the adsorption distribution trend of **C3G**$^+$ and Na^+ in compound **1,** respectively. The results display **C3G**$^+$ ions are mainly adsorbed in the cavities, while Na^+ ions can be adsorbed in the cavities and on the surface of compound **1** due to its small molecular size and high charge density. The adsorption capacity of Na^+ is higher than that of the **C3G**$^+$, which is further confirmed by the calculation results of the quantity of Na^+ ion and **C3G**$^+$ ion loading per unit cell, the calculated average Na^+ loading per unit cell of **1** is about 1800 at atmospheric pressure and temperature, while that is only 25 for **C3G**$^+$ ion due to its larger molecular size (Fig. S17). In addition, the calculated energy distribution of Na^+ and **C3G**$^+$ adsorbed by compound **1** are shown in Fig. S16. The energy distribution of **1** to adsorb **C3G**$^+$ is in the range of -260 ~ -150 kJ /mol and that is -1500 ~ -500 kJ /mol for Na^+, which indicates that the interaction between the anionic framework **1** and Na^+ ion is stronger than that of **C3G**$^+$ with the framework **1**, so Na^+ ions can easily exchange with **C3G**$^+$ ions in release experiments.

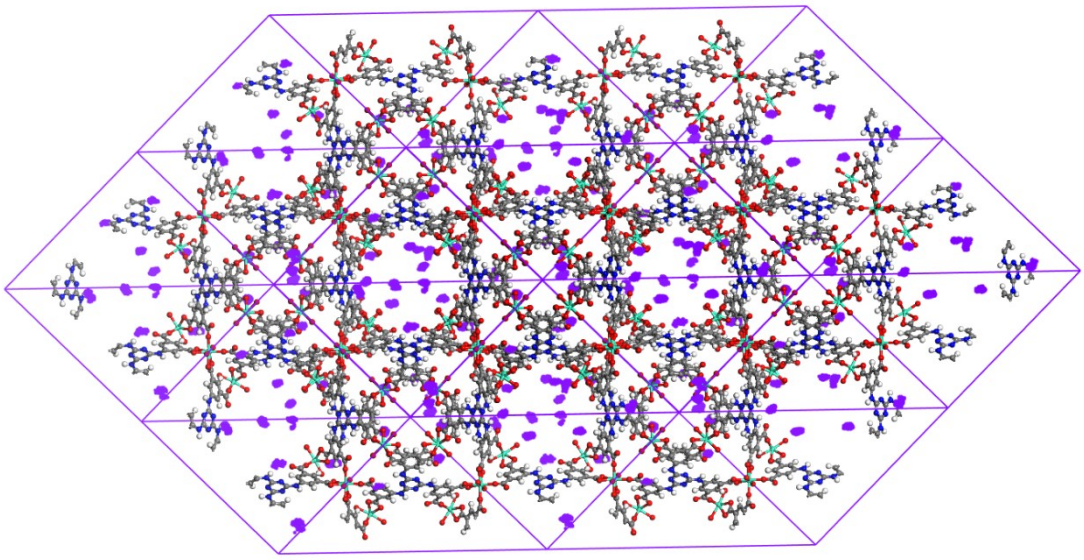

Fig. S14 The adsorption distribution trend of **C3G**$^+$ in compound **1**.

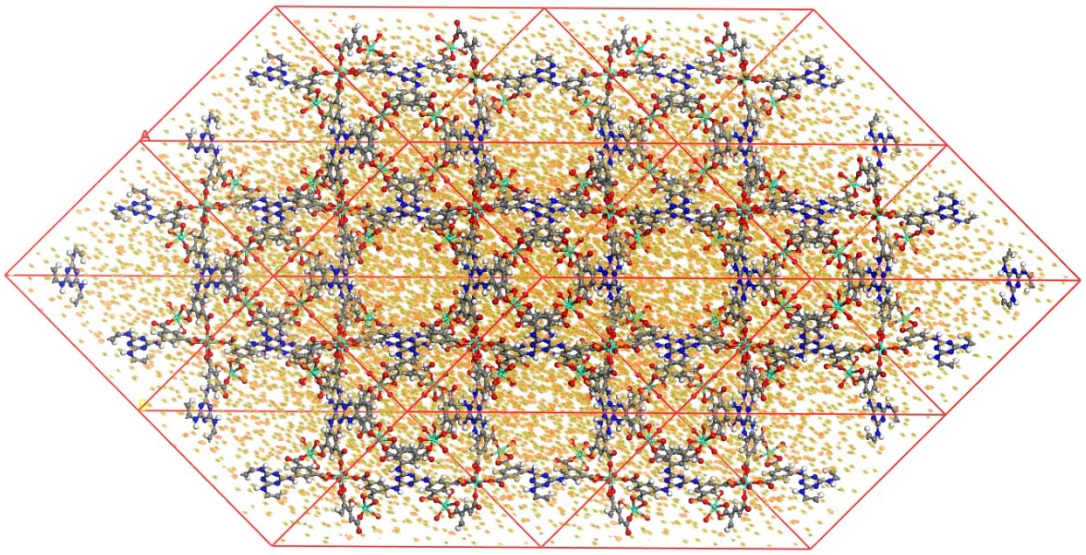

Fig. S15 The adsorption distribution trend of **Na**$^{+}$ in compound **1**.

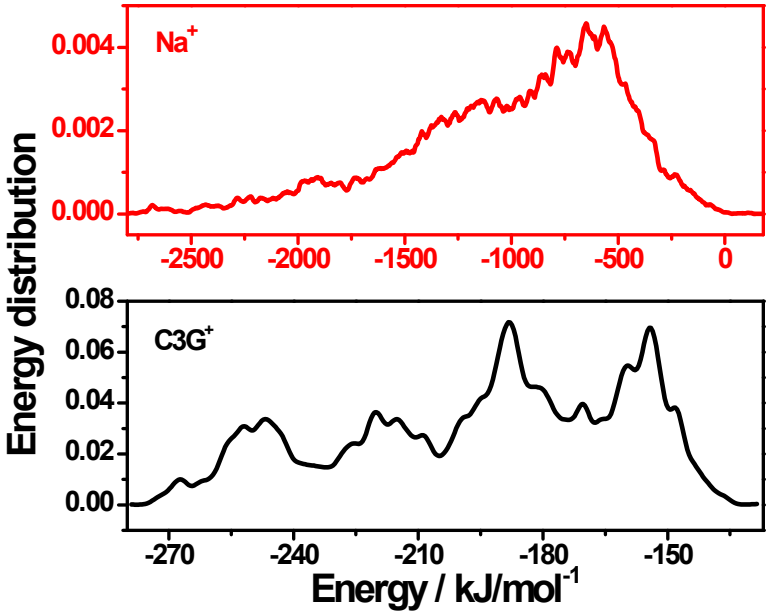

Fig. S16 The calculated energy distribution of Na^{+} and **C3G**$^{+}$ adsorbed by compound **1**.

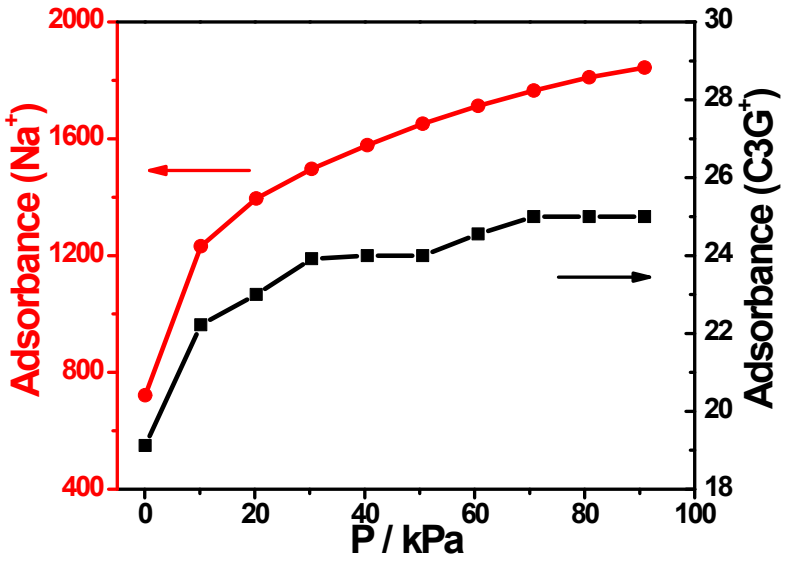

Fig. S17 The calculated energy distribution of Na^+ and **C3G**$^+$ adsorbed by compound **1**.

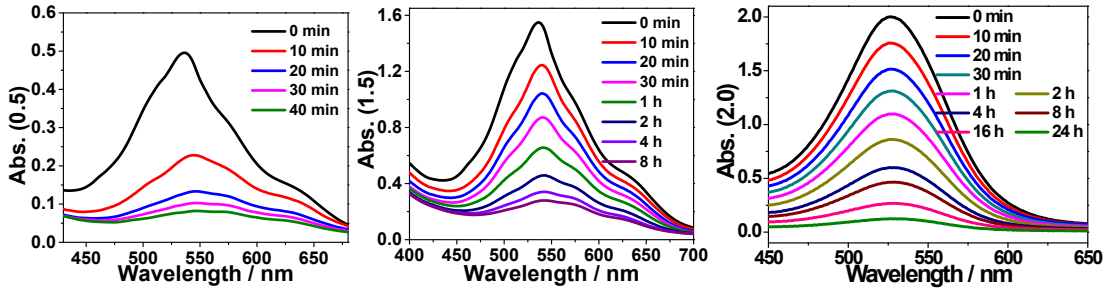

Fig. S18 Time dependent UV-vis spectra of 2 mL blackberry aqueous solution with the initial absorbance of about 0.5, 1.5 and 2.0 with 10 mg compound **1**.

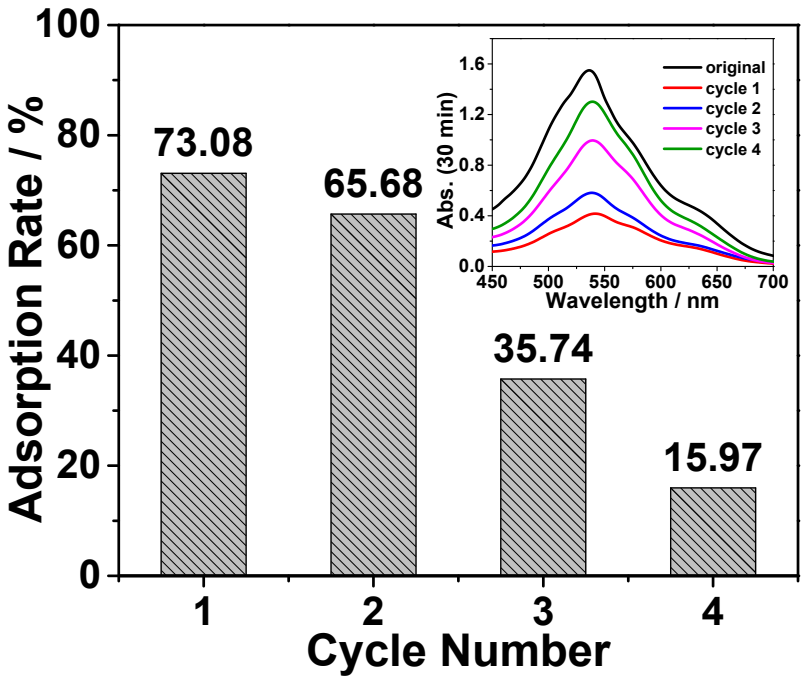

Fig. S19 The four cycles of adsorption rate of 2 mL blackberry aqueous solution with 30 mg compound **1** at 30 min. Inset, time dependence UV-vis spectra for four cycles.

The detection experiment of methyl viologen: 20 mg compound **1** were immersed in 10 mL aqueous solutions containing $\mathbf{MV^{2+}}$ with different concentrations (1×10^{-2}, 10^{-3}, 10^{-4}, 10^{-5}, 10^{-6}, 10^{-7}, 10^{-8} M) at room temperature for 10 min, respectively. The crystals were filtered and dried in air. Then the solid-state emission spectra of the obtained $\mathbf{MV^{2+}}$**@1** samples were measured on a Shimadzu RF-5310 under excitation at $\lambda_{ex} = 346$ nm.

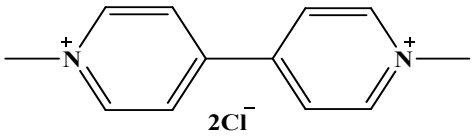

Fig. S20 The structure of methyl viologen ($\mathbf{MV^{2+}}$).

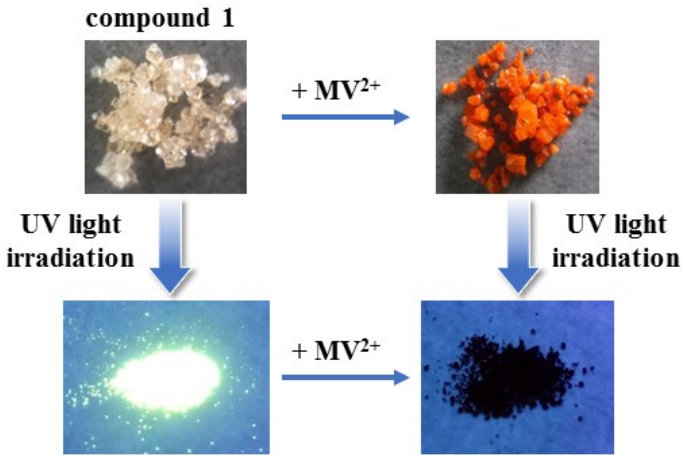

Fig. S21 The photos of crystals **1** before (left) and after (right) adsorption of $\mathbf{MV^{2+}}$ and their fluorescence under 365 nm UV light.

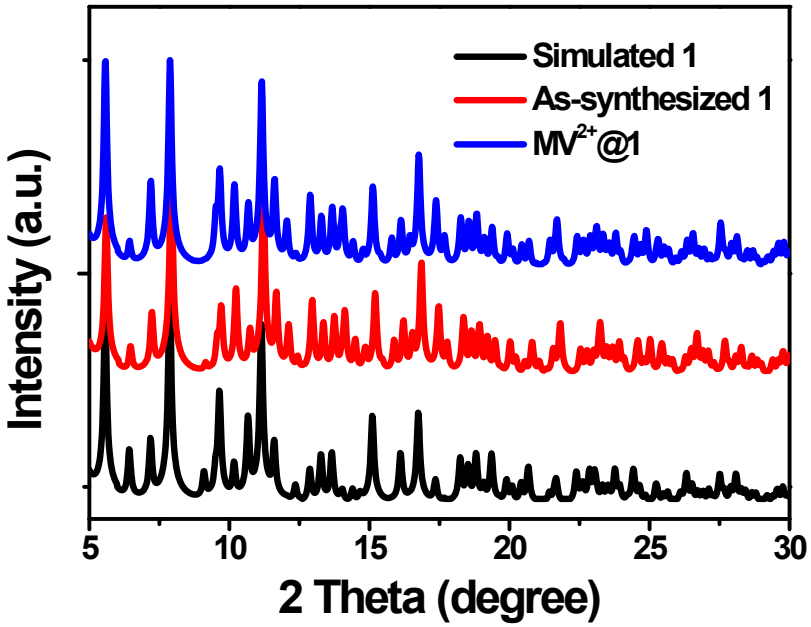

Fig. S22 The PXRD diffraction patterns of simulated, as-synthesized compound **1** and **MV^{2+}@1**.